Science
AAAS

An Evolving View of Saturn's Dynamic Rings
J. N. Cuzzi, *et al.*
Science **327**, 1470 (2010);
DOI: 10.1126/science.1179118

An Evolving View of Saturn's Dynamic Rings

J. N. Cuzzi,[1]*† J. A. Burns,[2]† S. Charnoz,[3] R. N. Clark,[4] J. E. Colwell,[5] L. Dones,[6] L. W. Esposito,[7] G. Filacchione,[8] R. G. French,[9] M. M. Hedman,[2] S. Kempf,[10] E. A. Marouf,[11] C. D. Murray,[12] P. D. Nicholson,[2] C. C. Porco,[13] J. Schmidt,[14] M. R. Showalter,[15] L. J. Spilker,[16] J. N. Spitale,[13] R. Srama,[10] M. Sremčević,[7] M. S. Tiscareno,[2] J. Weiss[13,17]

We review our understanding of Saturn's rings after nearly 6 years of observations by the Cassini spacecraft. Saturn's rings are composed mostly of water ice but also contain an undetermined reddish contaminant. The rings exhibit a range of structure across many spatial scales; some of this involves the interplay of the fluid nature and the self-gravity of innumerable orbiting centimeter- to meter-sized particles, and the effects of several peripheral and embedded moonlets, but much remains unexplained. A few aspects of ring structure change on time scales as short as days. It remains unclear whether the vigorous evolutionary processes to which the rings are subject imply a much younger age than that of the solar system. Processes on view at Saturn have parallels in circumstellar disks.

Saturn is encircled by an extensive ring system that, like the rings surrounding Jupiter, Uranus, and Neptune, resides within a region where tides from the parent planet frustrate aggregation of the ring particles into larger bodies (*1*). Several 1- to 100-km moons are interspersed within, and along, the peripheries of each of the four systems. Saturn's rings are distinguished by their far greater mass and by the purity of their icy particles, which is inconsistent with the unprocessed primordial mixture of ice, rock, and carbon-rich organics that make up the other ring systems. A bewildering diversity of structure permeates Saturn's main rings (Figs. 1 through 3) (*2*), which include the A ring, separated from the massive B ring by the Cassini Division—itself a ring—inward through the C ring and the nearly transparent D ring. A transition region beyond the A ring contains the complex, multistranded F ring, and arrayed yet farther outside the main rings are several diffuse rings composed of minute amounts of rubble and microscopic "dust." Within this diversity can be found structures that have analogs in the other three ring systems. Furthermore, the physics driving the evolution of Saturn's rings and determining their form has parallels with the processes active in protoplanetary disks.

The Voyager-era (1980s) perspective was that today's planetary ring systems cannot be primordial but must be continuously regenerated from their local arrays of moonlets, through vigorous evolutionary processes (*3*, *4*). To create Uranus' narrow rings, or the diffuse rings of Jupiter or Neptune, merely requires destroying a 1- to 10-km-diameter moonlet by impact with a heliocentric interloper. The ongoing evolution suggests that Saturn's rings, or parts thereof, might be only one-tenth the solar system's age, a greater challenge given their large mass. Just how Saturn's rings formed, and when, remain the most basic questions driving their exploration by the ongoing Cassini-Huygens mission [see Supporting Online Material (SOM) text 1]. An emerging perspective, after almost 6 years of study, is that Saturn's rings show dramatic variability on much shorter time scales—decades, years, even weeks.

Microstructure

The story of ring structure begins with dynamics at the smallest level: interactions between individual ring particles. Voyager and Earth-based occultations (*5*) revealed a broad ring-particle-size distribution extending from centimeters to meters in radius, well modeled by a power law having equal particle area per decade in radius (SOM text 2). Cassini's three-frequency radio occultations disclose rich radial variability in the abundance of the centimeter-size particles across the system (*6*). Rings B and inner A appear relatively devoid of these small particles compared with the C and outer A rings. Their abundance in outer ring A increases dramatically with ring radius. The very short lifetimes of particles in this size range to various evolutionary processes suggest that sizes are determined by an active accretion-destruction cycle (*7*, *8*) and are not primordial; thus, any radial variations indicate ongoing dynamics (*9*).

Particles closer to Saturn experience stronger gravity and move faster than those further out, generating Keplerian velocity shear across the ring. Collisions between particles, from a few to hundreds of times per orbit, are basic to local ring dynamics (*9*). Although the ring particles orbit Saturn at ~20 km/s, impacts occur at merely 0.01 to 0.1 cm/s. These collisions are inelastic, damping relative motions of the ring particles; this circularizes their orbits and flattens the system toward the planet's equator plane. Meanwhile, these small random motions are replenished by collisions and gravitational encounters with large particles and clumps of particles, ultimately deriving energy from the overall orbital motion. The vertical excursions of particles out of the plane arising from this small random velocity establish a ring thickness of a few tens of meters at most (SOM text 2) (*9*). In regions of low-to-medium optical depth, the ring kinetically behaves like a dense gas of macroscopic particles, with the random velocity corresponding to gas temperature; pressure and viscosity can be assigned to the ring material as well (see SOM text 2 to 4 for examples of liquid, or even solid, behavior). Most observed ring structure is created by the interplay between ring fluid dynamics and gravitational forces. Compared with other astrophysical disks (galaxies or protoplanetary disks), Saturn's rings are extremely thin (or dynamically "cold") owing to frequent inelastic collisions. Accordingly, the ring's self-gravity can be sufficiently strong compared to pressure forces to foster widespread, small-scale, gravitational instability.

Self-Gravity Wakes

The A ring's brightness has been observed to vary systematically with longitude (*10*, *11*). Motivated by studies of galactic disks, the underlying structure was explained by gravitational instabilities, where ring particles clump under their mutual self-gravity. In the A ring, Keplerian shear then stretches these clumps into elongated self-gravity wakes having a characteristic cant angle of 20° to 30° to the local orbital motion (Fig. 4 and SOM text 3). This clumping of particles, now scrutinized in Saturn's rings with Cassini observations, is analogous to planetesimal formation through gravitational instabilities in the protoplanetary disk (*12*). However, in the protoplanetary case, the surrounding nebular gas (missing in the rings) has much greater influence, whereas tidal forces have a lesser effect.

[1]Ames Research Center, NASA, Mail Stop 245-3, Moffett Field, CA 94035–1000, USA. [2]Department of Astronomy, Cornell University, Ithaca, NY 14853, USA. [3]Laboratoire Astrophysique Instrumentation Modélisation, Université Paris Diderot/Commissariat à l'Energie Atomique/CNRS, 91191 Gif sur Yvette Cedex, France. [4]U.S. Geological Survey, Denver, CO 80225, USA. [5]Department of Physics, University of Central Florida, Orlando, FL 32816, USA. [6]Department of Space Studies, Southwest Research Institute, Boulder, CO 80302, USA. [7]Laboratory for Atmospheric and Space Physics, University of Colorado, Boulder, CO 80309–0392, USA. [8]Istituto di Astrofisica Spaziale e Fisica Cosmica, Rome 00133, Italy. [9]Astronomy Department, Wellesley College, Wellesley, MA 02481, USA. [10]Max-Planck-Institut für Kernphysik, Saupfercheckweg 1, Heidelberg 69117, Germany. [11]Electrical Engineering Department, San Jose State University, San Jose, CA 95192, USA. [12]Astronomy Unit, Queen Mary University of London, London E1 4NS, UK. [13]Cassini Imaging Central Laboratory for Operations (CICLOPS), Space Science Institute, Boulder, CO 80301, USA. [14]Institute for Physics and Astronomy, University of Potsdam, Germany. [15]SETI Institute, Mountain View, CA 94043, USA. [16]Jet Propulsion Laboratory, California Institute of Technology, Pasadena, CA 91109, USA. [17]Carleton College, Northfield, MN 55057, USA.

*To whom correspondence should be addressed. E-mail: jeffrey.cuzzi@nasa.gov

†The first two authors led the manuscript's preparation; all others are listed alphabetically.

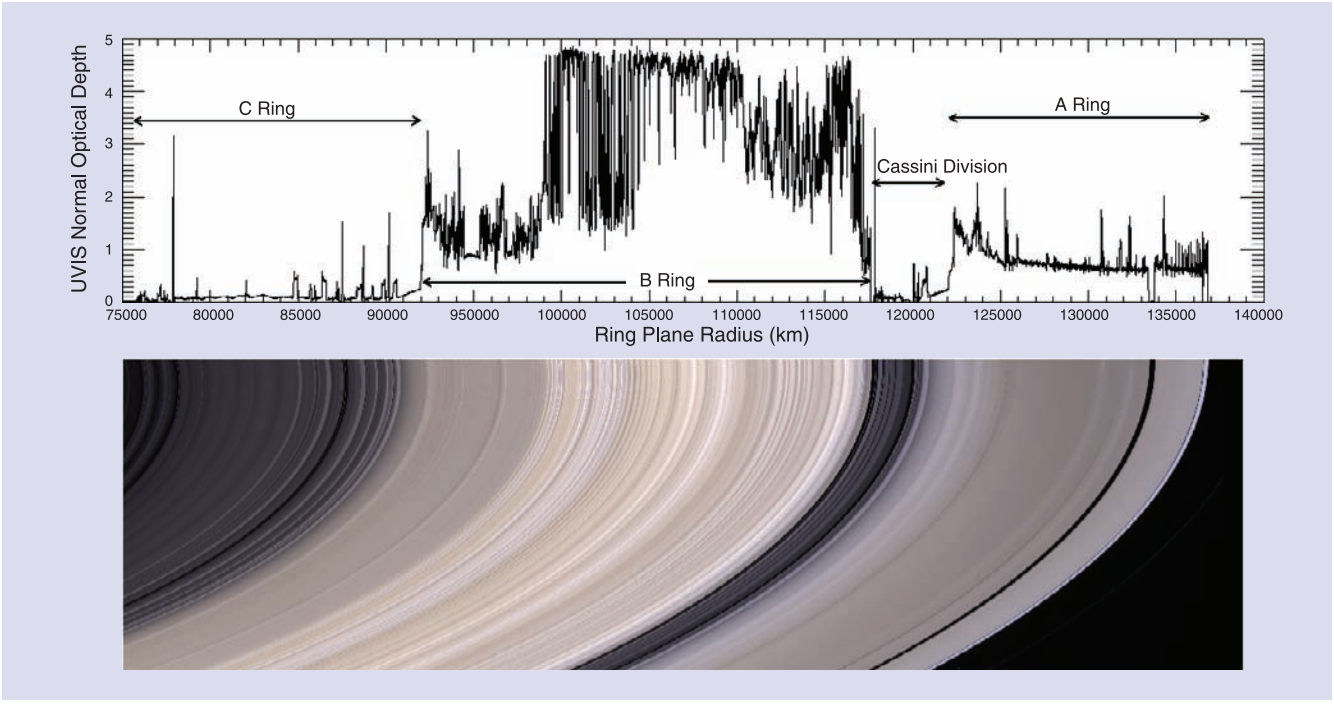

Fig. 1. An overview of Saturn's main ring system. (**Top**) Radial profile of ring optical depth from stellar occultations (*5*). (**Bottom**) True color image. The B ring—especially its dense central and outer portion—is filled with irregular structure that remains puzzling. The outer C ring contains a series of plateau features that are also not understood. The dark gap in the outer A ring is the Encke gap (Fig. 2), and the very narrow gap near the A ring's outer edge is the Keeler gap (Fig. 3). The identifiable brightness features in the A ring are spiral density and bending waves (Fig. 2). [Figure from (*11*).]

Cassini's stellar and radio occultations and images (*11*) have revealed self-gravity wakes to be ubiquitous throughout the A and B rings (but apparently absent elsewhere). That is, the rings consist of dense self-gravity wakes packed with particles, alternating with less densely populated gaps containing isolated particles. The light transmitted through the rings is thus controlled primarily by the gap sizes relative to the wakes, and secondarily by the optical depth of material within the gaps (*13*–*17*). In optically thick regions of the B ring, for example, the opaque wakes cover ~80% of the ring surface area, separated by gaps with a normal optical depth of ~0.2. Analysis of occultation data, using simple models for the wake's geometry, suggests a wake height of less than 10 m and in some regions below 5 m, indicating that the wakes are flattened relative to their lateral extent and consistent with direct measurements of ring edge thicknesses by occultations. Occultation data have been widely used to derive the ring's surface mass density, but the bulk of the ring mass may be concealed in these ubiquitous, opaque wakes (*18*) (SOM text 3).

Overstability

Organized, axisymmetric wave-like structures having only a few hundred meters radial length scale have been detected in the A and B rings (*14*, *19*, *20*). These features appear to be periodic and, in contrast to self-gravity wakes, show no measurable cant angle relative to the orbital direction. This axisymmetric structure may arise spontaneously from an oscillatory instability or "overstability" (*21*) if the ring's viscosity increases rapidly enough with its surface mass density (SOM text 4). Because the requisite density is present across most of the B ring, overstabilities were predicted throughout it (*21*–*23*). However, although Cassini radio occultation data (*20*) identify candidate structures routinely in the B ring, overstabilities are not always apparent. Thus, it remains unclear what could make parts of this ring overstable and others (with otherwise similar properties) not. Perhaps strong self-gravity wakes locally prevent overstability (*9*, *22*). In any case, the so-called "irregular structure" that permeates the entire B ring (*11*) (Fig. 1) has a radial scale ≥100 km, far too large to be explained by these overstabilities. Its cause remains unknown (see, however, our discussion of Ring Origin and Evolution below).

Spiral Density and Bending Waves

Saturn's satellites, orbiting beyond the rings or within ring gaps, can excite spiral waves at

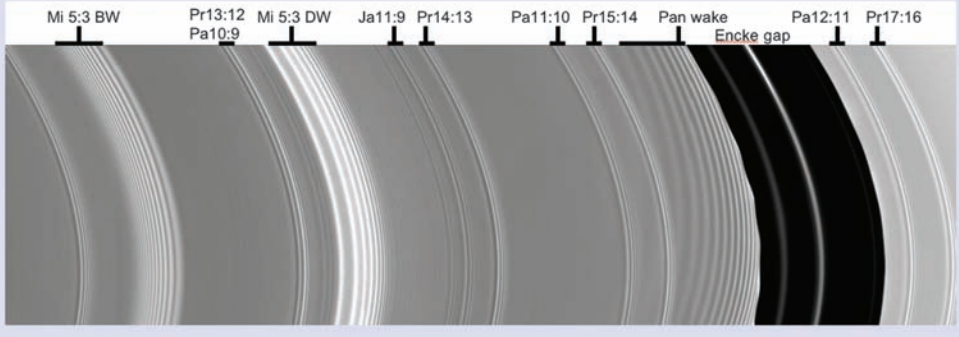

Fig. 2. A montage made from Cassini images, showing part of the outer A ring, including a prominent spiral bending wave and density waves (waves labeled by resonance, driven by Mimas, Pandora, Prometheus, and Janus), as well as the 320-km wide Encke gap (right), which contains several ringlets, one associated with the 10-km-radius embedded moonlet Pan that orbits in the gap's center. The wavy inner edge and the fan-shaped disturbance inside the edge result from the gravitational perturbations exerted on nearby ring material by Pan. By comparison with spiral waves in galaxies, the spiral density and bending waves are very tightly wrapped, like watch springs. [Figure from (*74*).]

CREDIT: MOSAIC, NASA/JPL/CICLOPS; ORIGINAL IMAGES, NASA/JPL/CICLOPS

locations where the orbital frequencies of ring particles are commensurate with those of the perturbing moons (SOM text 5). At these so-called resonances, ring particle orbits can be perturbed either within or perpendicular to their orbit planes, resulting in compression (density) or transverse (bending) disturbances, respectively. These disturbances are transmitted by the ring's local self-gravity, propagating as spiral waves until damped by viscous effects (*24*) (SOM text 5). Spiral bending waves (*25*) due to Mimas (Fig. 2) produce vertical corrugations in the ring with amplitudes as large as 1 km. After their prediction by analogy with galactic features, numerous spiral waves were detected by Voyager and Cassini, especially in the A ring (which, being closer to the perturbing moons, contains abundant resonant locations), but also in the B and C rings. Spiral waves in rings are more tightly wrapped than their galactic counterparts because the rings' mass is small compared to the central planet's mass.

The local surface mass density—a critical property for understanding ring evolution—is directly inferred from the wavelengths of spiral density and bending waves. The inner-to-mid-A ring is characterized by densities ~40 g/cm^2, whereas densities in the Cassini division are only a few g/cm^2 (*11*). Comparing the mass densities with the corresponding optical depths reveals substantial regional variations in the mean particle size (e.g., more small particles in the C ring and Cassini division), consistent with radio occultation results (*6*, *11*). The damping of spiral density waves measures the rings' viscosity, which arises from interparticle collisions plus Keplerian shear and increases outward in the A ring (*11*, *24*), which suggests a gradually increasing contribution of self-gravity wakes to the rings' total viscosity (*26*) (SOM text 2). The value of viscosity also constrains the rings' vertical thickness to 3 to 6 m in the Cassini division (*11*) and <10 to 15 m in the inner A ring (*24*).

The self-gravity wakes (Fig. 4 and SOM text 3) have radial wavelengths of 40 to 60 m, much less than those of the spiral density waves propagating through regions where they are common, so all material in the wakes should contribute to the surface mass densities calculated from the waves. Moreover, the wake lengthscale itself may be used to infer the local surface mass density, providing an independent check. The central B ring contains regions that are not sampled by spiral density waves. Thus the local surface mass density in the central B ring is essentially unconstrained and could be twice historical estimates (which are ~100 g/cm^2) or even more (*18*).

Spiral density waves transfer angular momentum between the rings and the forcing moons; thus, the orbits of the perturbing moons evolve outward, while those of the ring particles decay inward, at rates that limit the possible age of the ring-moon system. The magnitude of this effect (*27*) suggests that neither the A ring nor the close-in ring-moons could have retained their current separation for the solar system's age—one of two indications of youthful main rings. Cassini observations have validated the gravitational torque theory in the context of two embedded moonlets, where resonances merge (see below), even while recent work (*28*) has illuminated longstanding questions about how the moon Mimas constrains the B ring edge at its isolated 2:1 resonance (SOM text 6). Direct measurements of orbital evolution of the ring-moons under gravitational torques have been frustrated by dynamical chaos (*29*, *30*).

Embedded Moonlets

Embedded moons can open complete circumferential gaps in the surrounding nearby ring material by virtue of the gravitational torques transmitted at their closely spaced resonances (*27*) (SOM text 6). This was first demonstrated when Voyager data revealed the 14-km radius moonlet Pan in the Encke gap and further validated by Cassini's sighting of the 4-km radius moonlet Daphnis in the Keeler gap (SOM text 6). The equilibrium width of a moonlet-caused gap is obtained by balancing the moon's gravitational torque with the ring's viscous torque (*9*). The Encke gap's measured width is close to that predicted, and the relative scaling between the widths of the Keeler and Encke gaps is also roughly correct given the masses of Pan and Daphnis (*31*). These results support and constrain the widespread belief that Jupiter-mass objects can create cavities in circumstellar disks (*32*).

However, despite substantial campaigns by Cassini, moons have not yet been found inhabiting and clearing the other 13 named gaps in Saturn's rings. Five of the regularly spaced gaps in the Cassini division may be responding to subharmonics associated with the B ring's distorted edge (*28*); that edge, which oscillates in and out by as much as 75 km, appears to undergo unanticipated large angular librations or even circulations (*33*) relative to Mimas's longitude. Here the moving, nonaxisymmetric ring edge itself might play the role of a perturbing moonlet. Even if this explains the Cassini division gaps, the clearing of other nonresonant, apparently moon-free gaps, most in the C ring, remains baffling.

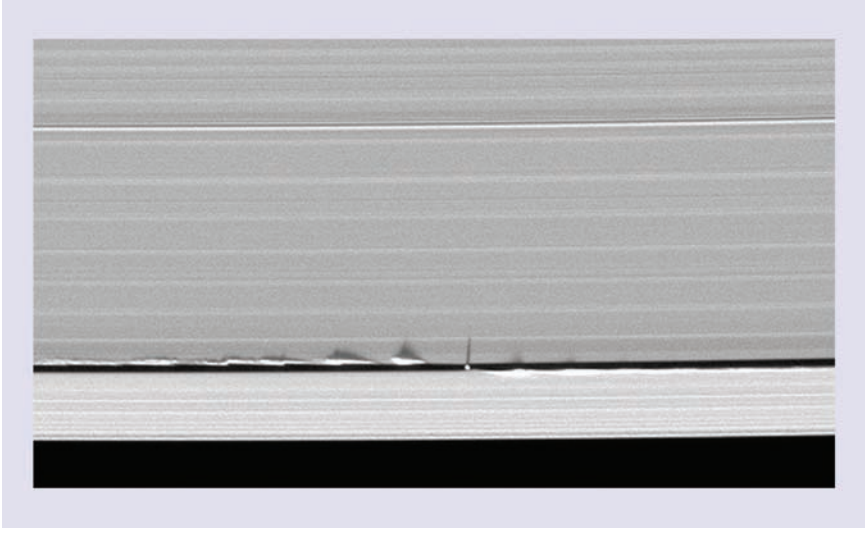

Fig. 3. Cassini image of the 30-km-wide Keeler gap at the A ring's very outer edge, showing its 4-km-radius embedded moonlet Daphnis along with the wake it creates in ring material at the gap edges. The image was taken very close to Saturn's equinox, with the sun at very low elevation, so that Daphnis and the wake's vertical relief cast shadows. The bright, narrow feature toward the top of the image is the Mimas 8:5 bending wave, whereas the other horizontal features include spiral density waves induced by Prometheus (most of the brighter, evenly spaced features) and Pandora; many density waves also have some vertical component, as indicated by their bright/dark appearance. [Figure from (*34*) with permission of the American Astronomical Society.]

Particles moving near a gap's edge are tugged as they pass the perturbing moon; their Keplerian shear, combined with the induced eccentric motion, produces a radial oscillation downstream of the moon whose period reflects the moon's distance and whose peak-to-peak amplitude measures the moon's mass. If the moonlet's orbit is sufficiently eccentric, or very close to the gap edge, nonlinear effects modify this result slightly (*34*, *35*). Collisions should cause the wavy edges to decay downstream, but the Encke edge's undulations persist around the full circumference, exhibiting the expected period and several others, too [see the figure in (*36*), taken from (*37*)]. Numerical simulations suggest that synchronization of orbit shapes in the densely packed

CREDIT: ORIGINAL IMAGE, NASA/JPL/CICLOPS

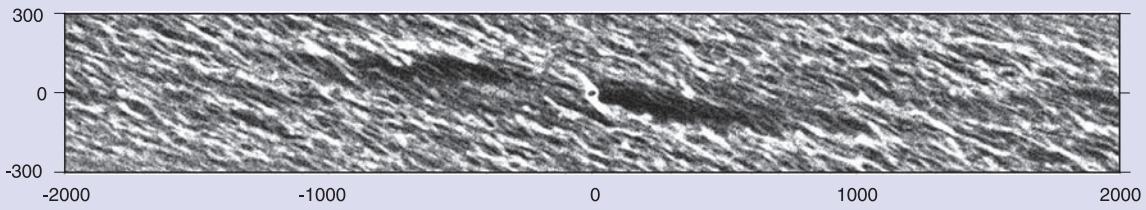

Fig. 4. This model calculation illustrates a "propeller" structure [the dark, mainly empty regions on either side of a 20-m-size object located at (0,°0)]. The slanted bright structures all around are self-gravity wakes (SOM Text 3). Objects causing propeller structures are too small to detect directly, but statistics on their sizes and distribution can be determined from detections of the disturbed regions on either side. [Figure from (*43*).]

moonlet wakes associated with these edge phenomena might forestall the expected decay (*35*) (SOM text 6). Cassini observations near Saturn equinox have shown that Daphnis' inclination drives wavy edges that oscillate vertically by 1 to 1.5 km along the Keeler gap's perimeters (Fig. 3) (*34*), whereas the Encke gap edges have undetectable vertical relief, consistent with Pan's lack of a measurable inclination.

Most of the moons that lie within or close to the rings—Pan to Pandora—display appreciably nonspherical forms, surprisingly low densities (substantially smaller than the density of solid water ice), and shapes and sizes that approximately match those of their associated Roche lobes (*38*), which suggests accretion of loose rubble onto a core substantially denser than the ambient ring material (*31*) (SOM text 6). This is reminiscent of numerical simulations of local gravitational aggregation of material in Saturn's rings (*39*) and is apparent in the ellipsoidal shapes of Phobos and Amalthea, close-in moons of Mars and Jupiter.

Packing in Compressed Regions

As ring material gets thrust together, in either the crowded crests of resonantly forced density waves, the wakes of passing moonlets, or perhaps the narrowed periapse regions of eccentric ringlets (SOM text 7), changes may occur in the particles' orbits and perhaps even their physical structures. The finite volumes of ring particles can also cause the ring material to "splash" vertically (SOM text 4) when compressed. Diverse particle orbits can be jammed into synchronized trajectories such that limited radial regions may orbit as units rather than with the normal Keplerian shear, reducing viscous dissipation and differential precession, and perhaps even creating large, clumpy structures (*35*) (SOM text 7). Disaggregation by disruptive collisions or tidal shedding (*7*) may follow. Images and occultations show broad swaths of "straw" in the innermost troughs between crests of strong spiral density waves (SOM text 7) and adjacent to the Encke gap edge (*19*, *35*). These clumps of "straw," probably formed by packing in the dense wave crests, are kilometers to tens of kilometers in extent. Whether this process leads to accretion of objects having some permanence remains unknown; propeller objects (see below) are absent from the regions surrounding the strongest density waves (*40*).

Propellers

Moonlets with sizes much smaller than Daphnis are unable to clear a complete circumferential gap, because their gravitational torques are too feeble to overcome viscous diffusion. However, they do create local disturbances that can be observed (Fig. 4 and SOM text 8). Such disturbances, shaped like propellers due to Keplerian shear, were predicted theoretically (*41*) and subsequently observed by Cassini (*40*, *42*, *43*). The central moonlets causing the disturbances remain unseen, but their sizes can be inferred from models of two azimuthally aligned lobes, with the leading (trailing) one offset slightly closer to (farther from) Saturn. The radial separation between the two lobes is a few times the central moonlet's diameter (*9*). Although the precise photometric and dynamical interpretations of the observations are controversial (SOM text 8), propeller moonlets appear to have radii from tens of meters to 1 km, with a much steeper size distribution than that of the centimeter- to few meter–sized particles that dominate the main rings (*40*, *42*, *43*). The total mass in these bodies is therefore relatively small.

Propellers seem to be largely confined to a 3000-km-wide band in the mid-A ring (*43*) that is divided into three sub-belts (*40*). Perhaps each sub-belt was produced by the local breakup of a larger object (*42*, *43*), or the propeller-rich belts are regions where accretion is enhanced and/or erosion is decreased (*40*). As inferred for Pan and Atlas (*31*), propeller moonlets may have grown to their current sizes by accretion of porous material onto a solid seed until the moonlet filled its own Roche lobe; the ultimate origin of these "seeds" remains unknown. Rarer and much larger propellers have been identified in the outer A ring, allowing individual objects to be tracked over extended times where some display evolving orbits (*44*). Continued monitoring of the orbital evolution of these propellers holds the promise of directly observing processes analogous to the complex evolution of a protoplanet through a circumstellar disk (*32*). A small (300 m) moonlet has been found in the outer B ring (*45*) but is missing its diagnostic propeller side lobes.

The F Ring

A dusty band of rubble orbiting 3000 km beyond Saturn's main rings, the F ring contains a long-lived core and several narrow peripheral strands, tens of km wide, that vary on time scales of hours to decades (*11*) (SOM text 9). A fainter dust belt spanning ~1500 km (*19*, *46*) surrounds the strands. Nearby Prometheus causes the primary perturbations, distorting the ring by tens of km at each passage (*46*, *47*). The phenomenon is analogous to the wakes produced by Pan and Daphnis but is complicated by the large variations in closest approach distance resulting from the orbital eccentricities of the ring and Prometheus (SOM text 9). For example, as Prometheus approaches and retreats from the ring each orbital period of 14.7 hours, its gravity repeatedly draws material out from the core to form a streamer, while leaving behind an emptier channel (*46*) (SOM text 9). The cycle recurs every 3.2° of longitude (i.e., the Keplerian shear over 14.7 hours), producing an obvious quasi-periodic pattern trailing Prometheus (Fig. 5). The strength of these perturbations peaks every ~19 years as differential precession brings the orbits of Prometheus and the F ring into antialignment; the closest approach between the pair occurred in late 2009.

Occasionally, more extraordinary events are observed. Within a few days, a ring sector's brightness can double or triple after a sudden injection of dust (*48*). Cassini images show that these features subsequently shear out to form kinematic spirals and "jets" (*47*, *49*) (Fig. 5). Even larger clumps have appeared in Hubble images (*50*), with orbits that apparently differ slightly from the F ring's core. The nearby object S/2004 S6 (*19*)—perhaps a ~5-km moonlet enshrouded in dust—is representative of several bodies that seemingly pass through the F ring semiregularly, and collisionally trigger these events (*47*, *49*, *51*). A particularly bright and dense structure appeared

in late 2007 with properties much like those of the main F-ring core but more than 100 km away in places (*52*) (SOM text 9).

The primary core of the F ring has an eccentric, inclined orbit that precesses smoothly (*52*, *53*), maintaining its integrity in seeming defiance of the large distortions and variations present, and, like Uranus's rings, avoiding differential precession as well. Because of the proximity of massive Prometheus and Pandora, which have numerous overlapping resonances, the dynamics of the F ring and nearby objects are more likely chaotic than shepherded (*54*). Stellar occultations have revealed opaque (or nearly opaque) bodies present throughout the ring's core, from 30 to 1200 m in diameter (*55*). These may be members of a previously unseen population of larger bodies that serve as dust sources and that provide the mass needed to stabilize the ring's orbit (*56*, *57*).

The F ring dramatically documents the difficulty of living near the edge of the Roche zone, where accretion and disruption are in continual combat (*1*, *39*). Understanding the evolution of the ring bodies, and their interactions with Prometheus, should provide a better grasp on the more general problem of protoplanets perturbing a disk of bodies from which they are also growing.

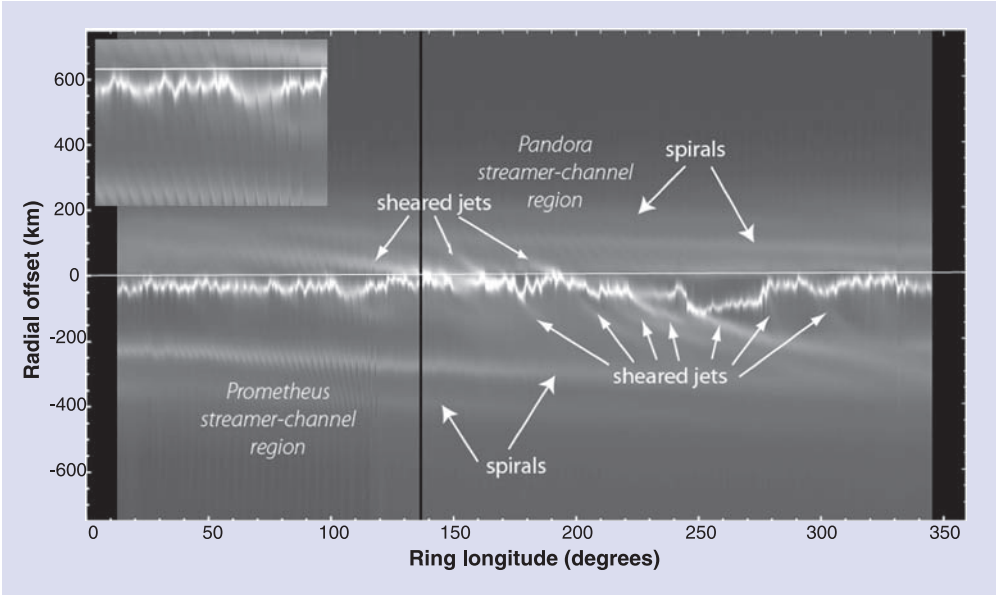

Fig. 5. A mosaic of reprojected Cassini ISS narrow-angle images of the F ring obtained at low phase angle. The radial offset is relative to a precessing elliptical model of the F ring (*52*, *53*), and the horizontal axis is the longitude (in degrees) at the epoch of 12:00 UTC on 1 January 2007. The mosaic is annotated to show the more prominent jets and spirals, thought to be due to recent collisions with a number of different crossing bodies, and the radially extended channels, which are caused by Prometheus and Pandora. As seen in the inset (expanded version of 75° to 125° longitude), most of the short-wavelength features in the bright core are due to perturbations from Prometheus (*11*, *47*, *49*). [Figure adapted from (*11*).]

CREDIT: ORIGINAL IMAGES, NASA/JPL/CICLOPS

Diffuse Rings

Saturn possesses several other low-optical-depth rings primarily containing micron-sized grains (*58*). Collisions happen infrequently in such systems, allowing nongravitational forces to be influential (*59*) (SOM text 10). These faint rings, and their analogs in the Jupiter, Uranus, and Neptune systems, may have parallels in circumstellar debris belts, whose apparently confined edges are considered to signify unseen planets (*60*).

Cassini observations have clarified the origins of many faint rings. Plumes of micron-sized grains emerging from warm fissures near Enceladus's south pole likely supply the extensive E ring (*58*, *61*, *62*). More commonly, dusty rings are fed by mutual collisions among, or meteoroid erosion of, various small parent bodies (*59*). Most of the moons interior to Enceladus's orbit (including Pan, Janus/Epimetheus, Pallene, Methone, and Anthe) generate faint rings or resonantly confined arcs of material in their orbits (*58*). The G ring is supplied from a resonantly trapped population of objects (including the 500-m Aegaeon) located near its inner edge (*63*, *64*). These dynamical configurations testify to the ubiquity of resonant trapping in faint debris disks. A Saturn-system-encircling dust ring has been detected by the Spitzer infrared telescope (*65*), with radial and vertical dimensions matching Phoebe's orbit; it too is a debris disk.

Some faint rings have changed appreciably since Voyager's visit (*66*). Both the D ring and inner C ring display a vertical corrugation that may have been generated only 25 years ago (*67*).

Ring Composition

The A and B ring particles are composed of >90 to 95% water ice, based on decades-old near-infrared spectra and radio/radar observations (*6*) (SOM text 11). Particles in the C ring and Cassini division are known to be dirtier, compatible with models of extrinsic pollution by carbon- and silicate-rich meteoroids over the rings' lifetimes (*68*). Cassini near-infrared observations have ruled out any CO_2, CH_4, or NH_3 ices at the percent abundance level, yet all of these species have been detected on Saturn's moons (SOM text 11). At wavelengths <520 nm, the A and B rings are much redder than any of Saturn's icy moons; the ultraviolet (UV) absorber responsible for this remains a puzzling clue to the rings' origin. Cassini identifies no near-infrared C-H spectral feature in the rings, which might preclude some large, reddish, organic tholins as possible absorbers (*69*). Two new candidates have been suggested: small clusters of carbon rings (polycyclic aromatic hydrocarbons) and/or Fe^{3+} compounds such as nanoparticles of iron oxide, which gives Mars its ruddy color. The idea of "rusty rings" was inspired by Cassini's identification of the rings' oxygen atmosphere and their spectral dissimilarity to supposedly organic-rich reddish icy solar system objects (*6*). The degree of visual redness is highly correlated with water-ice band strengths as a function of radius (*70*)—with redness and ice band depth increasing together in the more massive ring regions, suggesting that the UV absorber is distributed intrinsically, within the ice grains in the regolith of the ring particles, rather than as a distinct, or extrinsic, component.

Ring Origin and Evolution

Arguments that the rings may be just one-tenth as old as the solar system are (i) mutual repulsive density-wave torques between (primarily) the A ring and the nearby ring-moons and (ii) meteoroid restructuring and pollution of the ring material (SOM text 12). These short lifetimes are problematic because the generation of the entire ring through disruption of a Mimas-size (or larger) parent is unlikely on this time scale (*3*, *71*, *72*).

However, loopholes remain in the young-ring arguments. The gravitational torque theories on which (i) depends have now been validated by observations of moonlets clearing gaps. Some flexibility in their implications for ring age may emerge if ring-moons periodically interact and perhaps temporarily destroy each other (*73*) or are held up by much-sought-for, but as-yet-unidentified, resonances with exterior massive moons (*27*). Pollution contaminates the entire system, but models rely on the poorly known incoming mass flux and ring mass (SOM text 12). Any substantial increase in the rings' mass could make them better able to withstand the effects of meteoroid bombardment. Firm mass

measurements from density waves now blanket most of the rings, but the murky depths of the B ring may contain considerably more material than previously believed (SOM text 12).

We remain unsure whether the propeller objects (or even the visible gap-moons Pan and Daphnis) are residual shards from a creation event or locally grown. Are the large peripheral ring-moons (at least Prometheus and Pandora) examples of ring precursors, or were they grown within the A ring and repelled outwards by their gravitational interaction with the ring? Is the F ring the detritus of some more recently destroyed member of this tribe, and/or does accretion continue there as well?

The composition of the main rings, and its variation with radius, might yet be the best clue as to the provenance of their predecessor(s); however, one must first unravel the various evolutionary processes affecting composition (the ring atmosphere, meteoritic pollution, and the like) and structure. Yet, much of the ring's structure—the irregular structure covering the B ring; the crisp, symmetrical, banding in the C ring; and the Cassini division itself—remains unexplained (see, however, SOM text 12).

We have learned a great deal about the rings in the decades since Voyager, from ground-based observations and theoretical modeling, and in particular during Cassini's nearly 6 years at Saturn. Far more remains to be done. By mission's end, Cassini will return hundreds of times more data than Voyager, and careful examination of this data set is still in its early stages. Explanations for the origin of Saturn's rings will remain unconvincing until we have understood the powerful dynamical processes that have formed, and continue to shape, these elegant structures on time scales reaching from yesterday to billions of years.

References and Notes

1. R. M. Canup, L. W. Esposito, *Icarus* **113**, 331 (1995).
2. The "optical thickness" or "optical depth" τ of a ring of randomly distributed particles is defined as $\tau = \int n(r)\, \pi\, r^2\, dr$, where $n(r)$ is the vertically integrated number density per radius increment for particles of radius r, and we have assumed that the ring particles are much larger than the wavelength of light. For small number densities, this is effectively the projected surface area of particles per unit ring area. Usually this is expressed as the "normal" optical depth, corresponding to rays arriving perpendicular to the mean plane of the rings.
3. A. W. Harris, in *Planetary Rings*, R. Greenberg, A. Brahic, Eds. (Univ. Arizona Press, Tucson, 1984), pp. 641–659.
4. S. Charnoz, L. Dones, L. W. Esposito, P. R. Estrada, M. M. Hedman, in *Saturn from Cassini-Huygens*, M. K. Dougherty, L. W. Esposito, T. Krimigis, Eds. (Springer Netherlands, 2009), pp. 535–573.
5. In an occultation, the signal from a star (Cassini observes occultations in ultraviolet and infrared radiation) or the spacecraft (its microwave transmission) is "occulted" when the source passes behind the rings as seen by the observer. The source's spatial footprint on the rings is the smeared Fresnel-zone size (geometric mean of the wavelength and distance from the rings to the observer) and is generally tens of meters, comparable to the size of the typical largest ring particles. Thus, stellar and radio occultations are key tools in ascertaining ring microstructure.
6. J. N. Cuzzi *et al.*, in *Saturn from Cassini-Huygens*, M. K. Dougherty, L. W. Esposito, T. Krimigis, Eds. (Springer Netherlands, 2009), pp. 459–509.
7. D. R. Davis, S. J. Weidenschilling, C. R. Chapman, R. Greenberg, *Science* **224**, 744 (1984).
8. P.-Y. Longaretti, *Icarus* **81**, 51 (1989).
9. J. Schmidt, K. Ohtsuki, N. Rappaport, H. Salo, F. Spahn, in *Saturn from Cassini-Huygens*, M. K. Dougherty, L. W. Esposito, T. Krimigis Eds. (Springer Netherlands, 2009), pp. 413–458.
10. The A-ring quadrants preceding the two longitudes aligned with an observer are up to tens of percent dimmer than the other two. The exact amplitudes depend on wavelength and the elevations of the observer and of the Sun as seen from Saturn.
11. J. E. Colwell *et al.*, in *Saturn from Cassini-Huygens*, M. K. Dougherty, L. W. Esposito, T. Krimigis, Eds. (Springer Netherlands, 2009), pp. 375–412.
12. E. Chiang, A. Youdin, *Annu. Rev. Earth Planet. Sci.* (2010); http://arjournals.annualreviews.org/doi/abs/10.1146/annurev-earth-040809-152513
13. J. E. Colwell, L. W. Esposito, M. Sremčević, *Geophys. Res. Lett.* **33**, L07201 (2006).
14. J. E. Colwell, L. W. Esposito, M. Sremčević, G. R. Stewart, W. E. McClintock, *Icarus* **190**, 127 (2007).
15. M. M. Hedman *et al.*, *Astron. J.* **133**, 2624 (2007).
16. P. D. Nicholson, M. M. Hedman, *Icarus*, in press. Published online 28 July 2009; 10.1016/j.icarus.2009.07.028.
17. M. S. Tiscareno *et al.*, *Astron. J.* **139**, 492 (2010).
18. S. J. Robbins, G. R. Stewart, M. C. Lewis, J. E. Colwell, M. Sremčević, *Icarus*, in press. Published online 26 September 2009; 10.1016/j.icarus.2009.09.012
19. C. C. Porco *et al.*, *Science* **307**, 1226 (2005).
20. F. S. Thomson, E. A. Marouf, G. L. Tyler, R. G. French, N. Rappaport, *Geophys. Res. Lett.* **34**, L24203 (2007).
21. U. Schmit, W. M. Tscharnuter, *Icarus* **115**, 304 (1995).
22. H. Salo, J. Schmidt, F. Spahn, *Icarus* **153**, 295 (2001).
23. J. Schmidt, H. Salo, F. Spahn, O. Petzschmann, *Icarus* **153**, 316 (2001).
24. M. S. Tiscareno, J. A. Burns, P. D. Nicholson, M. M. Hedman, C. C. Porco, *Icarus* **189**, 14 (2007).
25. F. H. Shu, J. N. Cuzzi, J. J. Lissauer, *Icarus* **53**, 185 (1983).
26. H. Daisaka, H. Tanaka, S. Ida, *Icarus* **154**, 296 (2001).
27. P. Goldreich, S. Tremaine, *Annu. Rev. Astron. Astrophys.* **20**, 249 (1982).
28. M. M. Hedman *et al.*, *Astron. J.* **139**, 228 (2010).
29. R. G. French, C. A. McGhee, L. Dones, J. J. Lissauer, *Icarus* **162**, 143 (2003).
30. P. Goldreich, N. Rappaport, *Icarus* **166**, 320 (2003).
31. C. C. Porco, P. C. Thomas, J. W. Weiss, D. C. Richardson, *Science* **318**, 1602 (2007).
32. J. E. Chambers, *Annu. Rev. Earth Planet. Sci.* **37**, 321 (2009).
33. This terminology follows that for a vertically hanging pendulum, where "libration" refers to oscillations about the stable (minimum energy) location and "circulation" describes a complete cycle through the stable point.
34. J. W. Weiss, C. C. Porco, M. S. Tiscareno, *Astron. J.* **138**, 272 (2009).
35. M. C. Lewis, G. R. Stewart, *Icarus* **178**, 124 (2005).
36. J. A. Burns, J. N. Cuzzi, *Science* **312**, 1753 (2006).
37. M. S. Tiscareno *et al.*, *Bull. Am. Astron. Soc.* **37**, 767 (2005).
38. The Roche lobe is the region of space that is gravitationally bound to a body, balancing the effects of its orbital and rotational motions and the parent planet's tides.
39. R. Karjalainen, H. Salo, *Icarus* **172**, 328 (2004).
40. M. S. Tiscareno, J. A. Burns, M. M. Hedman, C. C. Porco, *Astron. J.* **135**, 1083 (2008).
41. F. Spahn, M. Sremčević, *Astron. Astrophys.* **358**, 368 (2000).
42. M. S. Tiscareno *et al.*, *Nature* **440**, 648 (2006).
43. M. Sremčević *et al.*, *Nature* **449**, 1019 (2007).
44. M. S. Tiscareno *et al.*, *Bull. Am. Astron. Soc.* **41**, 559 (2009).
45. C. C. Porco, Cassini Imaging Team, *IAU Circ. 9091* (2009).
46. C. D. Murray *et al.*, *Nature* **437**, 1326 (2005).
47. C. D. Murray *et al.*, *Nature* **453**, 739 (2008).
48. M. R. Showalter, *Icarus* **171**, 356 (2004).
49. S. Charnoz *et al.*, *Science* **310**, 1300 (2005).
50. C. A. McGhee, P. D. Nicholson, R. G. French, K. J. Hall, *Icarus* **152**, 282 (2001).
51. S. Charnoz, *Icarus* **201**, 191 (2009).
52. N. Albers *et al.*, *Bull. Am. Astron. Soc.* **40**, 430 (2008).
53. A. S. Bosh, C. B. Olkin, R. G. French, P. D. Nicholson, *Icarus* **157**, 57 (2002).
54. O. C. Winter, D. C. Mourão, S. M. Giuliatti-Winter, F. Spahn, C. da Cruz, *Mon. Not. R. Astron. Soc.* **380**, L54 (2007).
55. L. W. Esposito, B. K. Meinke, J. E. Colwell, P. D. Nicholson, M. M. Hedman, *Icarus* **194**, 278 (2008).
56. J. N. Cuzzi, J. A. Burns, *Icarus* **74**, 284 (1988).
57. J. M. Barbara, L. W. Esposito, *Icarus* **160**, 161 (2002).
58. M. Horanyi, J. A. Burns, M. M. Hedman, G. Jones, S. Kempf, in *Saturn from Cassini-Huygens*, M. K. Dougherty, L. W. Esposito, T. Krimigis, Eds. (Springer Netherlands, 2009), pp. 511–536.
59. J. A. Burns, D. P. Hamilton, M. R. Showalter, in *Interplanetary Dust*, E. Grün, B. A. S. Gustafson, S. F. Dermott, H. Fechtig, Eds. (Springer-Verlag, Berlin, 2001), pp. 641–725.
60. J. M. Carpenter *et al.*, *Astrophys. J.* **181**, (Supp.), 197 (2009).
61. C. C. Porco *et al.*, *Science* **311**, 1393 (2006).
62. F. Postberg *et al.*, *Nature* **459**, 1098 (2009).
63. M. M. Hedman *et al.*, *Science* **317**, 653 (2007).
64. C. C. Porco, Cassini Imaging Team, *IAU Circ. 9023* (2009).
65. A. J. Verbiscer, M. F. Skrutskie, D. P. Hamilton, *Nature* **461**, 1098 (2009).
66. M. M. Hedman *et al.*, *Icarus* **188**, 89 (2007).
67. M. M. Hedman, J. A. Burns, M. M. Tiscareno, C. C. Porco, *Bull. Am. Astron. Soc.* **41**, 1042 (2009).
68. J. N. Cuzzi, P. R. Estrada, *Icarus* **132**, 1 (1998).
69. F. Poulet, D. P. Cruikshank, J. N. Cuzzi, T. L. Roush, R. G. French, *Astron. Astrophys.* **412**, 305 (2003).
70. P. D. Nicholson *et al.*, *Icarus* **193**, 182 (2008).
71. J. J. Lissauer, S. W. Squyres, W. K. Hartmann, *J. Geophys. Res.* **93** (B11), 13776 (1988).
72. L. Dones, *Icarus* **92**, 194 (1991).
73. F. Poulet, B. Sicardy, *Mon. Not. R. Astron. Soc.* **322**, 343 (2001).
74. L. Lovett, J. Horvath, J. Cuzzi, *Saturn: A New View* (H. N. Abrams, New York, 2006).

75. We applaud with gratitude the Cassini spacecraft engineering and operations teams. We thank the other members of the Cassini Rings Discipline Working group for their many contributions, not all of which could be described here. We thank our Ring Science Planning Team leaders at JPL—B. Wallis, K. Perry, C. Roumeliotis, R. Lange, and S. Brooks—and the observation planning and design specialists on all the teams represented here for their essential contributions to the mission's success. We acknowledge M. Lewis, H. Salo, and G. Stewart for the simulations and visualizations described in the SOM and for helpful comments. We also thank three anonymous reviewers, R. E. Johnson, R. Pappalardo, P. Kalas, and C. Niebur for helpful suggestions on presentation. The U.S. authors were supported by NASA through the Cassini Project and Cassini Data Analysis Program. Other support was provided by the Italian Space Agency (ASI), Deutsches Zentrum für Luft und Raumfahrt (DLR), the Newton Institute, Université Paris Diderot and CEA-Saclay, and the U.K. Science and Technology Facilities Council.

Supporting Online Material

www.sciencemag.org/cgi/content/full/327/5972/1470/DC1
SOM Text
Figs. S1 to S9
Table S1
References
Movies S1 to S7

10.1126/science.1179118